Renewable and Sustainable Energy Reviews 16 (2012) 5848–5860

Contents lists available at SciVerse ScienceDirect

Renewable and Sustainable Energy Reviews

journal homepage: www.elsevier.com/locate/rser

Review on dye-sensitized solar cells (DSSCs): Fundamental concepts and novel materials

Jiawei Gong [a], Jing Liang [b], K. Sumathy [a,*]

[a] Department of Mechanical Engineering, North Dakota State University, Fargo, USA
[b] Department of Polymer Science, East China University of Science and Technology, Shanghai, PR China

ARTICLE INFO

Article history:
Received 31 August 2011
Received in revised form
22 April 2012
Accepted 28 April 2012
Available online 9 August 2012

Keywords:
Dye-sensitized solar cells
Nanocrystalline semiconductor films
Charge transfer
Sensitizers
Electrolyte

ABSTRACT

The prosperity of human society largely relies on safe energy supply, and fossil fuel has been serving as the most reliable energy source. However, as a non-renewable energy source, the exhaustion of fossil fuel is inevitable and imminent in this century. To address this problem, renewable energy especially solar energy has attracted much attention, because it directly converts solar energy into electrical power leaving no environment affect. In the past, various photovoltaic devices like organic, inorganic, and hybrid solar cells were fabricated in succession. In spite of high conversion rate of silicon based solar cells, the high module cost and complicated production process restricted their application solely to astronautic and aeronautic technology. For domestic and other commercial applications, research has been focused on organic solar cells for their inherent low module cost and easy fabrication. In addition, organic solar cells have their lightweight and flexibility advantage over conventional silicon-based crystalline solar cells. Among all the organic solar cells, dye-sensitized solar cells (DSSCs) are the most efficient and easily implemented technology. Here, this study examines the working principle, present development and future prospectus for this novel technology.

Contents

1. Introduction

Nobel laureate Richard Smalley listed energy and environment problems on the top of challenges that we will face in next 50

* Corresponding author. Tel.: +1 701 231 7139.
E-mail address: sumathy.krishnan@ndsu.edu (K. Sumathy).

1364-0321/$ - see front matter © 2012 Elsevier Ltd. All rights reserved.
http://dx.doi.org/10.1016/j.rser.2012.04.044

Nomenclature

k_B	Boltzmann constant, equal to 1.38066×10^{-23} J K^{-1}
Φ_0	incident photoflux (cm^{-2} s^{-1})
T	absolute temperature
e	elementary charge, equal to 1.60218×10^{-19} C
n_0	electron density on the conduction band of TiO_2 in the dark (cm^{-3})
η	quantum yield of photogenerated electron/photoelectric conversion efficiency
k_{et}	recombination reaction rate
R_f	roughness factor
M	electrical mobility
μ_H	Hall mobility

Subscripts

oc	open circuit
sc	short circuit

years. The increase in energy consumption has accelerated the depletion of the earth's oil reserves, and the combustion exhaust of fossil fuels has resulted in the environmental contamination and greenhouse effect. Currently, worldwide concerns of such problems significantly spur the technological endeavor of renewable and green energy. The European Union (EU) has set a goal that by 2020 renewable energy should account for 20% of the EU's final energy consumption (10.3% in 2008) [1]. In accordance, the American Recovery and Reinvestment Act in the United States has budgeted more than $80 billion in clean energy development aiming to reduce greenhouse gas emission by 28% by 2020 [2]. At present, a clear trend has been observed as the renewable energy share of global energy consumption in 2008 is 19%, which is a 50% increase compared to the 13% in 2003 [3,4].

Among all the renewable energy forms, solar energy has showed its advantages and potential for power generation. Solar radiation amounts to 3.8 million EJ/year, which is approximately 10,000 times more than current energy needs [5]. From the perspective of energy conservation and environmental protection, it is desirable to directly convert solar radiation into electrical power by the application of photovoltaic devices. It is shown in Fig. 1, in the 5-year period between the end-2004 to 2009, solar photovoltaic energy generation has increased at 60% annual growth rate, fastest among all the renewable technologies [4].

High cost and complicated production process exclude traditional silicon-based solar cells from the domestic and other commercial applications. However, in recent decades several organic solar cells have been invented that combine the lightweight and flexibility of organic molecules with the low module cost [6,7]. In terms of efficiency and easy fabrication, the dye-sensitized solar cell is one of the most promising alternatives to the silicon solar cells.

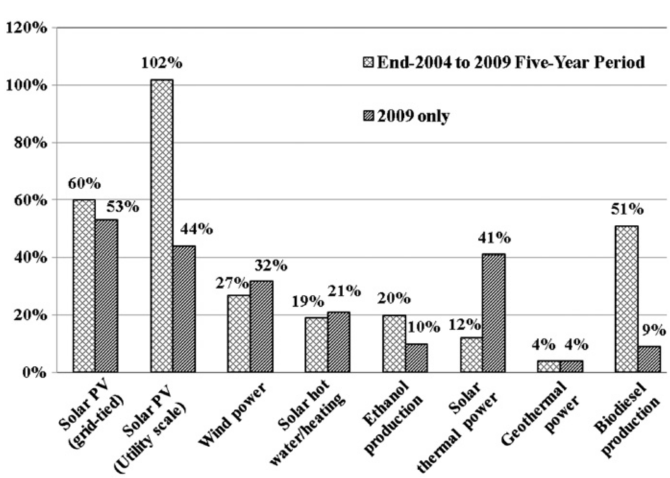


Fig. 1. Average annual growth rates of renewable energy capacity, the end-2004–2009 [4].

In 1991, Oregan and Grätzel built the first dye sensitized nanocrystalline solar cells whose photoelectric energy conversion rate reached 7.1% and incident photon to electrical current conversion efficiency was approximately 80% [8]. This simple structure and low cost technology have further stimulated great research interest to improve the efficiency of dye-sensitized solar cells which has attained ca. 10% [9], a level deemed as necessary for commercial use [10].

2. Operational principle of the dye-sensitized solar cell

Dye-sensitized solar cell (DSSC) is a semiconductor photovoltaic device that directly converts solar radiation into electric current. The operational principle of DSSC is illustrated in Fig. 2. The system consists of the following:

(i) a transparent anode made up of a glass sheet treated with a transparent conductive oxide layer;
(ii) a mesoporous oxide layer (typically, TiO_2) deposited on the anode to activate electronic conduction;
(iii) a monolayer charge transfer dye covalently bonded to the surface of the mesoporous oxide layer to enhance light absorption;
(iv) an electrolyte containing redox mediator in an organic solvent effecting dye-regenerating; and
(v) a cathode made of a glass sheet coated with a catalyst (typically, platinum) to facilitate electron collection.

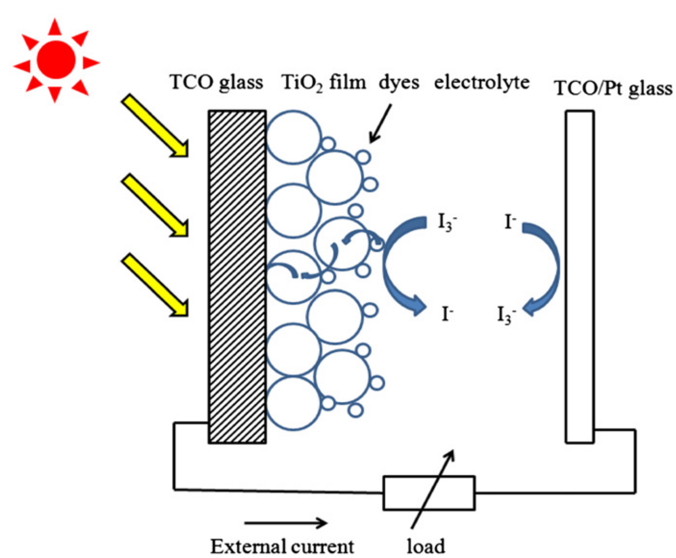


Fig. 2. Schematic diagram of the dye-sensitized solar cell.

When exposed to sunlight, the dye sensitizer gets excited from which an electron is injected into the conduction band of the mesoporous oxide film. These generated electrons diffuse to the anode and are utilized at the external load before being collected by the electrolyte at cathode surface to complete the cycle.

In order to enhance electrical conductivity and light transmittance, conducting glass is used as the substrate. There are mainly two types of conducting glass: indium-doped tin oxide (ITO) and fluorine-doped tin oxide (FTO). The standard to select a proper type is sometimes ambiguous because of the variety of cell configurations and materials [11]. The semiconductor electrode is usually a layer of nanocrystalline titanium dioxide (TiO_2), a thin film deposited on the conducting glass film with the thickness ca. 5–30 μm, which plays an important role in both the exciton dissertation and the electron transfer process. The porosity and morphology of the TiO_2 layer are dominant factors that determine the amount of dye molecules absorbed on its surface which can provide an enormous area of reaction sites for the monolayer dye molecules to harvest incident light. A large number of artificial dye molecules have been synthesized since the first introduction of dye-sensitized solar cells and some of them have already been successfully commercialized such as N3, N719 and Z907. Desirable dye molecules have to meet certain criteria, such as match with the solar spectrum, long-term operational stability, and firm graft on the semiconductor surface. In addition, their redox potential should be high enough to facilitate the regeneration reaction with a redox mediator [12]. As such, iodide and triiodide (I^-/I_3^-) redox couple is most commonly used in the liquid electrolyte, while other solid-state and quasi-solid electrolytes like organic hole-transport material and polymer gel are also applicable [13–17]. Platinum is generally used as the cathode to catalyze the reduction of the oxidized charge mediator [18].

The overall performance of the above described solar cell can be evaluated in terms of cell efficiency (η) and fill factor (FF) expressed as

$$FF = \frac{V_{max}J_{max}}{V_{oc}J_{sc}} \tag{1}$$

$$\eta = \frac{V_{oc}J_{sc}\,FF}{P_{in}} \times 100\% \tag{2}$$

where J_{sc} is the short-circuit current density (mA cm^{-2}), V_{oc} the open-circuit voltage (V), and P_{in} the incident light power. J_{max} and V_{max} correspond to current and voltage values, respectively, where the maximum power output is given in the *J–V* curve.

In the band gap theory, the difference between the quasi-Fermi level of the TiO_2 layer and the electrolyte redox potential determines the maximum voltage generated under illumination. As shown in Eq. (3) the open-circuit voltage varies with the iodide concentration because the recombination reaction occurs between the electrons on the conduction band of TiO_2 and I_3^- (triiodide) [19].

$$V_{oc} = \frac{kT}{q}\ln\left(\frac{\eta\Phi_0}{n_0 k_{et}[I_3^-]}\right) \tag{3}$$

where η is the quantum yield of photogenerated electron for the given incident photoflux (Φ_0); n_0 represents the electron density on the conduction band of TiO_2 in the dark, while k_{et} reflects the recombination reaction rate for the given triiodide concentration $[I_3^-]$.

Similarly, the precise value of J_{sc} can be calculated by integrating the product of incident photon to current efficiency (IPCE) and incident photoflux (Φ_0) over the spectral distribution, expressed as

$$J_{sc} = e\int \mathrm{IPCE}(\lambda)\Phi_0(\lambda)(1-r(\lambda))d\lambda \tag{4}$$

where '*e*' is the elementary charge and $r(\lambda)$ is the incident light loss. One prominent approach to improve the circuit current density (J_{sc}) is to increase the IPCE value by utilizing panchromatic dyes which can absorb incident light at a longer wavelength.

Yet another parameter that influences the efficiency of the DSSC is the fill factor (FF) which is associated with the electron transfer process and internal resistance of dye-sensitized solar cells. A variety of equivalent circuits have been elaborated to interpret data obtained from electrochemical impedance spectroscopy [20,21]. Based on the equivalent circuit study, it is shown that FF can be optimized by minimizing internal series resistance.

3. Panchromatic sensitizer

As mentioned above, the ideal sensitizer has to meet several requirements that guide effective molecular engineering: (i) the sensitizer should be able to absorb all incident light below the near-IR wavelength of approximately 920 nm; (ii) it must carry a carboxylate or phosphonate group to anchor on the surface of semiconductor oxide; (iii) the lowest unoccupied molecular orbital (LUMO) of the sensitizer must match to the edge of the conduction band of the oxide to minimize the energetic potential losses during the electron transfer reaction; (iv) the highest occupied orbital (HOMO) of the sensitizer must be sufficiently low to accept electron donation from an electrolyte or a hole conductive material; (v) it should be stable enough to endure 10^8 turnovers corresponding to 20 years exposure to sunlight without apparent degradation.

Since its discovery in 1993 [22], *cis*-RuL_2-$(NCS)_2$ (N3 dye) has become the paradigm of the efficient charge-transfer sensitizer for nanocrystalline TiO_2 films. It has an absorption threshold around 800 nm covering the visible to the near-infrared region of solar spectrum. In addition, in N3 dye can inject photoexcited electrons into the semiconductor layer efficiently via carboxylate groups which on the one hand firmly attach to the surface of TiO_2 as an electron transfer channel, and on the other hand link to the bipyridyl moiety to lower the energy of the ligand π* orbital. Since the molecular electronic transition is a metal-to-ligand charge transfer, this structure is energetically favored in the electron injection process. The performance of N3 dyes as a sensitizer is almost unmatched until the emergence of black dye. Nazeeruddin et al. [23] first reported the synthesis of a class of black dye which displays the panchromatic sensitization character over the whole visible range extending from the near-IR region up to 920 nm. Later conversion efficiency utilizing black dye was certified to be 10.4% by the Swiss Federal Institute of Technology in Lausanne (EPFL) [24]. Recently, by using black dye N749, Chiba et al. [25] could achieve the highest recorded overall efficiency of approximately 11.1% with an area of 0.219 cm [2] under standard AM 1.5 illumination. Until now, the photovoltaic performance of black dyes is expected to be superior to all other known charge-transfer sensitizers in terms of the whole range light absorption [26]. Incident photon to current conversion efficiency (IPCE) comparison between N3 and N749 is presented in Fig. 3. It is observed that the spectrum response of black dye extends ca. 100 nm wavelength to 900 nm the infrared region than that of N3 dye, which covers more near-IR region of the sunlight spectrum leading to a high IPCE value.

Though ruthenium (II) based dyes have provided a relatively high efficiency, there are several drawbacks of them: the high cost and the limited amount of noble metals, and also the sophisticated synthesis and purification steps. To address these issues, metal-free organic dyes have been prepared and applied in DSSCs to replace Ru (II) based dyes [27].

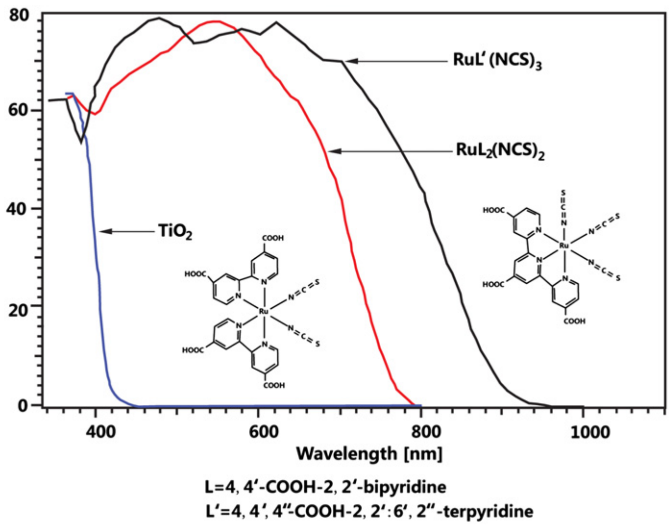


Fig. 3. Incident photo to current conversion efficiency (IPCE): chemical structures of the sensitizers are shown as insets [26].

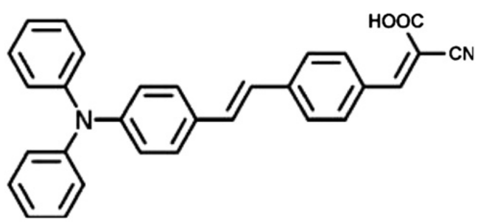


Fig. 4. Molecular structure of TA-St-CA dye [28].

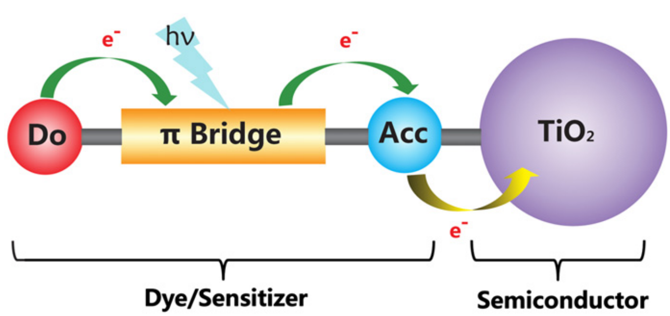


Fig. 5. Design structure of metal-free organic dyes [27].

At present, an overall solar-to-energy conversion efficiency 9.1% has been obtained by Hwang et al. [28] based on an organic metal-free dye TA-St-CA shown in Fig. 4. It contains a p-conjugated oligo-phenylenevinylene unit with an electron donor–acceptor moiety for intramolecular charge transfer and a carboxyl group as an anchoring unit for the attachment onto TiO_2 nanoparticles. This configuration can be generalized as the donor-π bridge-acceptor structure shown in Fig. 5, which implies an essential design principle for metal-free dyes. Guided by this design principle, Yella et al. [29] synthesized a donor-π bridge-acceptor zinc porphyrin dye (YD2-*o*-C8) which suppresses the interfacial electron back transfer from the nanocystalline TiO_2 film to the oxidized cobalt mediator, and leads to a strikingly high power conversion efficiency of 12.3% under simulated air mass 1.5 global sunlight.

Another possible route to produce cost-effective dyes on a large scale is to extract natural dyes from plant sources. Natural dyes have many advantageous features such as their cost-efficiency, non-toxicity, and complete biodegradation [30]. Although currently a device incorporating natural dyes has a much lower efficiency than those using synthesized dyes, it is noticeable that via structural modification, the natural dyes can have a performance as good as, if not better than their synthesized counterparts [31]. Thus, the structural optimization of natural dyes is a promising way to improve device efficiency.

4. Semiconductor photoanode

Semiconductors such as TiO_2, ZnO, SnO_2, and chalcogenides have been under extensive investigation due to their wide application in energy storage and environmental remediation. They act as sensitizers to facilitate light-reduced redox processes because of their conductive electronic structure, referred to as valence band (VB) and conduction band (CB). Band positions of several commonly used semiconductors are shown in Fig. 6. In the quantum physics theory, a photon with energy ($h\nu$) that exceeds or matches the band gap (E_g) of a semiconductor can excite an electron to the conduction band leaving a hole with a positive charge at the valence band. These charges can either be transferred to the external circuit to provide electrical current or be utilized to catalyze a certain chemical reaction [32].

4.1. Semiconductor oxide film

Titanium dioxide (TiO_2) exits in three natural forms namely rutile, anatase and brookite. Among them the most stable form is rutile, which is at the equilibrium phase for any temperature. Though rutile form is more stable, anatase is perceived to be more chemically active when used in dye-sensitized solar cells. Anataseis metastable and has a trend to convert to rutile upon heating. Hence, the phase constituents are greatly influenced by the synthesis processing method. Nowadays, the commercial product DeGussa P25 has 80% anatase and 20% rutile at about 25 nm. In order to study this phase conversion influence, experiments were conducted to compare dye-sensitized rutile- and anatase-based TiO_2 solar cells [33]. Dye-sensitized solar cells (DSSCs) fabricated with rutile and anatase films at the same thickness were subjected to the simulated AM 1.5 solar illumination. Results show essentially the same value of open-circuit voltage (V_{oc}), whereas the short-circuit photocurrent (I_{sc}) of the anatase-based cell is 30% higher than that of rutile-based cell. The difference in short-

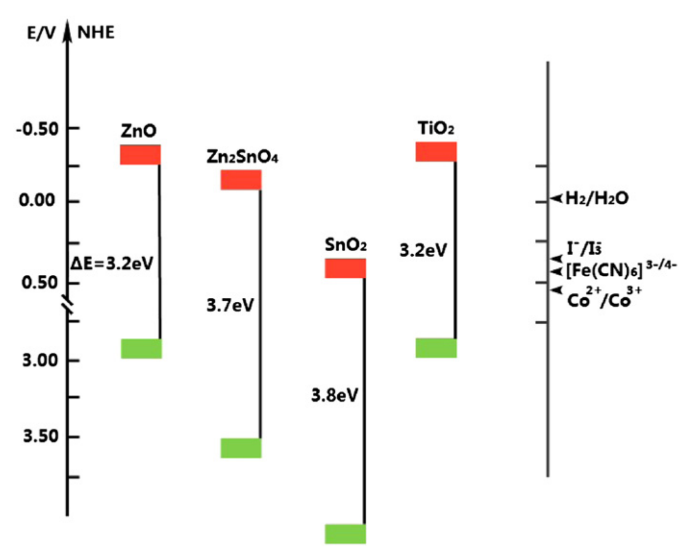


Fig. 6. Band positions of several semiconductors and potentials of redox couples are represented using normal hydrogen electrode as reference.

circuit current is attributed to the lower amount of dye absorption by the rutile film, owing to a relatively smaller specific surface area. The electron transfer rate in rutile film is generally slow in nature due to the low coordination number associated with the particle packing density, which is identified by intensity-modulated photocurrent spectroscopy.

Fig. 6 shows that various semiconductor oxides have similar energy band structure as that of TiO_2. The structure similarity makes them not only a possible substitute to TiO_2 in DSSCs, but also brings their own unique characteristic towards it. Intensive research has been dedicated to investigate this issue and potential application in other regimes. Zinc oxide (ZnO) is a promising alternative to TiO_2 because of the similar band structure and relatively high electron mobility (1–5 $cm^2 V^{-1} s^{-1}$) [34]. Redmond et al. [35] reported the first transparent nanocrystalline ZnO films prepared on a conducting glass substrate by sol–gel techniques. They are sensitized by *cis*-RuL_2-$(NCS)_2$ (N3 dye) and incorporated as the light-harvesting unit in a regenerative photoelectronchemical cell. The resulting device has a monochromatic IPCE of 13% at 520 nm and a simulated AM 1.5 solar conversion efficiency of 0.4%. This low efficiency is mainly due to the dissolution of the ZnO surface and formation of Zn^{2+}/dye aggregates in the acidic N3 solution. Later on, such obstacles are overcome by adding a base (KOH) to the acidic loading solution [36] or immersing the ZnO film in ethanolic solution under reflux [37]. Currently, Saito and Fujihara [38] fabricated ZnO photoanodes by a squeegee method and obtained the highest overall light-to-electric conversion efficiency of 6.58% under AM 1.5 with a large short-circuit photocurrent density of 18.11 mA cm^{-2}.

Tin dioxide (SnO_2) is another attractive option having two main advantages over TiO_2: high mobility, and large band gap. At room temperature 300 K, SnO_2 electron mobility (ca. 100–200 $cm^2 V^{-1} s^{-1}$ [39]) was measured by Fonstad and Rediker [40] which is three orders higher than that of TiO_2 (ca. 0.1–1 $cm^2 V^{-1} s^{-1}$) [41]. The larger band gap of SnO_2 (3.8 eV), compared to TiO_2 (3.2 eV), would create fewer oxidative holes in the valence band under ultraviolet illumination, thereby reducing the dye degradation rate and improving the long time stability of DSSCs. More positive band edge position facilitates electron injection from photoexcited dye molecules [42]. However, surprisingly the performance of dye-sensitized solar cells based on SnO_2 is so far much less than that based on TiO_2 [43]. The inferior photovoltaic properties of SnO_2 are ascribed to the faster electron recombination dynamics resulting from a 100-fold higher electron diffusion constant at matched electron densities, and from a 300 mV positive shift of the SnO_2 conduction band [44]. In addition, the lower isoelectric point (IEP) of SnO_2 (pH 4–5), compared with TiO_2 (pH 6–7), inhibit the adsorption of dye molecules with acidic carboxyl groups [45]To overcome the above issues, conformal isolating oxide layers such as TiO_2, ZnO, MgO, and Al_2O_3 are coated on the surface of SnO_2 photoanode to suppress the back reaction, which can significantly improve the photoconversion efficiency. As reported by Senevirathna et al. [46], the maximum overall light-to-electrical efficiency of about 7% can be achieved by MgO-coated SnO_2 DSSCs.

Tan et al. [47] first synthesized large band gap energy (3.6 eV) ternary oxides Zn_2SnO_4 nanoparticles with desirable particle size from a hydrothermal process and tested it in the DSSCs. It could achieve an overall light-to-electrical conversion efficiency of about 3.8% under AM 1.5 illumination. This efficiency is comparable to that of the single component ZnO solar cell (4.1%) [48], and such Zn_2SnO_4 is more stable than ZnO against acidic dyes. Currently, the short electron diffusion length remains a limiting factor for the performance of Zn_2SnO_4 cells. These results are further confirmed by Huang et al. [48] who used Zn_2SnO_4 as electrode materials for the metal-free indoline DSSCs. Though prone to the low electron transfer and enhanced charge recombination, nanocrystalline TiO_2 has been regarded as the paragon of semiconductors since 1991. Up to now, no other material could replace its leading role in either research or commercial applications.

4.2. Transparent conducting substrate

Apart from semiconductor oxide film, the transparent conducting substrates also play an important role in dictating the DSSCs' performance. They are thin layer films that function as a current collector and a support of the semiconductor layer in DSSCs. They have two important features: the high optical transparency which allows natural sunlight to pass through to the beneath of the active material without unwanted absorption of the solar spectrum, and the low electrical resistivity which facilitates electron transfer process and reduces energy loss.

Indium tin oxide (ITO, In_2O_3:Sn) films exhibit an ideal transparency (transmittance over 80%) and resistivity (ca. $10^{-4}\ \Omega$ cm) at room temperature, so they are widely used as transparent conducting oxide in the field of optoelectronic device. It is notable that depending on the preparation method, the electrical properties of ITO films disperse widely. As reported by Tahar [49], In_2O_3:Sn synthesized from $In_2(SO_4)_3 \cdot nH_2O$ and $SnSO_4$ by dipping method has the resistivity of $6–8 \times 10^{-4}\ \Omega$ cm. The low resistivity is believed to be the result of the large free carrier densities caused by (i) substitution of indium atom by tin atom releasing one extra electron, and (ii) oxygen vacancies acting as two electron donors [50,51]. However, their low resistivity property could be deteriorated during the calcinations process in the DSSCs fabrication.

Typical fabrication of the photoelectrodes in DSSCs involves coating and sintering TiO_2 pasta on conducting substrates at high temperature ca. 450 °C to improve the electronic contact [8]. When ITO film is exposed to high temperature above 300 °C, the sheet resistance increases drastically, leading to very low device efficiency. Such increased resistance can be explained by the reduced carrier density. When ITO films annealed at high temperature, oxygen in the atmosphere starts to fill the oxygen vacancies which function as an electron supplier. To prevent the loss of charge carriers in high temperature, a double layer structure has been utilized to achieve the thermal stability of ITO-based substrates. The thin layer metal oxides, such as ATO (SnO_2:Sb antimony-doped tin oxide), AZO (aluminum-doped zinc oxide), and SnO_2 have been sputtered onto the ITO surface to form the double layer which has proved to be a much better structure than single layer ITO [52].

Apart from the listed transparent conducting oxides, fluoride-doped tin oxide (SnO_2:F, FTO) with a similar structure and working principle as ITO has been attempted. FTO-coated glass substrates have 70–80% transmittance in the visible range at a thickness of 750 nm, approximately 10% less than that of ITO substrates. The sheet resistance of FTO coated glass is $< 12\ \Omega/\Box$, about 20% lower than that of ITO coated glass (15 $\Omega/\Box$). Above all, for the comparable transparency and conductivity, FTO-coated glass costs less than one-third of ITO-coated glass [53].

Studies have been conducted to compare the performance of ITO and FTO based DSSCs by Sima et al. [11]. They fabricated DSSCs in a standard configuration and TiO_2/TCO/glass layers were subjected to thermal treatment at 450 °C for 2 h in an oxygen atmosphere. It was found that the sheet resistance value of ITO increased from the original 18 $\Omega/\Box$ to 52 $\Omega/\Box$ after the thermal treatment, whereas sheet resistance of FTO remained unchanged at the value of 8.5 $\Omega/\Box$. The cell based on ITO substrate has an overall cell efficiency of 2.24%; in contrast, an identical cell based on FTO has an efficiency of 9.6%. This experimental comparison

correlating the sheet resistance to cell efficiency has confirmed that the ITO substrate is unstable when subjected to high temperature.

Although widely used, the traditional ITO and FTO based transparent conducting oxide appears to be increasingly problematic due to the following:

- the limited availability and high cost of the rare earth element indium,
- their sensitivity to thermal treatment and pH environment,
- their limited transparency in the near-infrared region, and
- mechanical brittleness [54].

Recently, ultrathin graphene films have been used in solid state DSSCs as an alternative to ITO and FTO. As reported by Wang et al. [55], these graphene films obtained by reducing graphite oxide on the surface of the substrates show a high conductivity of 550 S/cm and a transmittance of more than 70% over 1000–3000 nm. Although cell efficiency based on graphene film is much lower (0.26%) than that of FTO-based cells, there are still several favorable characteristics that indicate graphene as a promising candidate, such as the outstanding chemical and thermal stability, and ultrasmooth surface with tunable wettability [56].

4.3. Contact optimization

The three phase contact between ITO, TiO_2, and electrolyte in DSSCs plays a crucial role in photoelectron transfer and recombination dynamics. It is clear that the transport of extracted photoelectron in TiO_2 conduction band has to be transferred effectively to the ITO substrates in order to affect high cell efficiency. Therefore, methods have to be established to suppress the electron recombination during the transfer process.

There are mainly two recombination mechanisms: the electrons recombine with the holes in the excited dye molecules; and the electrons reduce the triiodide to iodide ion. In fact, these two chemical reactions occur concurrently as competing reactions. Research has been done to compare their reaction kinetics with the photoelectron injection process. It was found that recombination between photoinjected electrons with oxidized dye molecules or I_3^- ions occurs in microseconds (10^{-6} s) [57,58]. Asbury et al. [59] observed that the electron transfer dynamics between the excited dye molecules into the TiO_2 conduction band is on the femtosecond (10^{-15} s) scale by femtosecond mid-IR spectroscopy, whereas I^- ions reduce the oxidized dye on 10^{-8} seconds scale. Because the reduction rate of dye molecules is two orders of magnitude faster than the recombination with photoelectrons, the contribution of the former mechanism can usually be neglected. The dominant recombination reaction is represented by the reaction:

$$I_3^- + 2e \rightarrow 3I^- \quad (5)$$

Because the electrolyte can penetrate through the mesoporous TiO_2 layer all the way to the ITO substrates, back electron transfer occurs on surface of both TiO_2 and ITO substrate. One of the successful approaches to suppress the detrimental recombination is to develop a blocking layer on the oxide electrode material.

There exist various types of blocking layers made of semiconductors and insulating materials such as TiO_2, Nb_2O_5, ZnO, $CaCO_3$ and $BaCO_3$. They are tested for their effectiveness in the DSSCs. Among them, the compact TiO_2 layer seems to be the most suitable candidate because it not only alleviates the back electron transfer on the FTO surface, but also provides a larger contact area between TiO_2/FTO to enhance the electron transfer as shown in Fig. 7 [60]. Cameron and Peter [61] investigated the influence of the blocking layers on the back transfer of electrons to tri-iodide

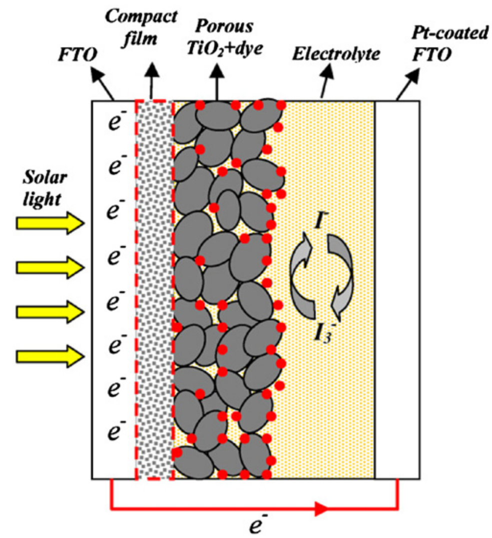


Fig. 7. Schematic diagram of the DSSC with a compact TiO_2 layer [60].

ions by open circuit photovoltage decay. The results show that the blocking layer effectively prevents the back reaction of electrons with tri-iodide ions in the electrolyte, especially under short circuit conditions.

It is commonly assumed that the back electron transfer on the FTO substrate can be neglected under short-circuit condition because the I_3^- to I^- exchange current density is negligibly small. The major electron recombination takes place on the surface of TiO_2 mesoporous network because its surface area is much larger than that of FTO. Fortunately, suppression of back electron transfer in TiO_2 has been achieved by passivating recombination centers with 4-tertbutylpyridine [62]. Besides, organic sensitizer with long chain alkoxy groups is found to effectively reduce the recombination rate, most likely by inhibiting the access by redox mediator to the TiO_2 surface [29].

4.4. Morphology influence

4.4.1. Mesoporous films

Mesoporous materials have pores between 2 and 50 nm in diameter. They usually have a continuous network that can either be ordered or disordered resulting in high internal surface area. Such structure is favorable in heterogeneous chemical reactions because it provides a sufficient surface as reaction sites and facilitates mass diffusion by internal channels. The first dye-sensitized solar cells (DSSCs) [8] based on the mesoporous TiO_2 films achieved a remarkable breakthrough. Till recently, the mosoporous film is regarded as the most favorable electrode structure and widely used as a standard to study DSSCs. Unique characteristics are found in mesoporous TiO_2 compared with its compact analogs: the low inherent film conductivity, no built-in electrical field within nanocrystalline particles, and three dimensional semiconductor/electrolyte interface contact [63]. Mesoporous film, though it yields extremely high specific surface area for dye uptake, could enhance the charge recombination to triiodide ions on the TiO_2/electrolyte interface. Thus, it is advantageous to have thinner films.

The mesoporous structure of the film depends on the preparation method, and its pore size distribution can be adjusted, for example, by controlling molar ratio of stearic acid to titanium tetraisopropoxideas precursor [64]. Barbé et al. studied the microstructure of the mesoporous film correlation with preparation conditions such as precursor chemistry, temperature for hydrothermal growth, binder addition, and sintering conditions

influence [65]. The film morphology and network geometry have a great influence on the electron transport dynamics of DSSCs. The correlation between film morphology and photoelectrochemical performance of DSSCs was investigated by Saito et al. [66]. It is reported that the amount of dyes adsorbed and photocurrent generated under illumination were proportional to the roughness factor (R_f) under 1400, and the diffusion limit of electrolyte rarely affected the photocurrent under 1 sun irradiance. Benkstein et al. [67] found the electron diffusion coefficient D has a power-law dependence on the film: $D \propto |P - P_c|^{\mu}$, where the critical P_c is 0.76 ± 0.01 and the conductivity exponent μ is 0.76 ± 0.05. It is shown that an increase in porosity shifts the distribution of coordination numbers of the particles to a low value, indicating a tortuous transport pathway and increased dead ends in the TiO_2 film.

Recently, a novel TiO_2 mesoporous network with multilayer structure was designed by Wang et al. [68]. In their work, multilayer films with different sized particles (diameter from ca. 100 nm to 23 nm) were fabricated and aligned layer by layer on the conducting glass to enhance light scattering. This structure effectively increased the IPCE at the red region and led to high cell efficiency 10.2%.

4.4.2. High order nanostructure

As mentioned in Section 4.4.1, the conductivity of mesoporous film is much lower than its bulk analog. The electron diffusion coefficient determined by laser lash-induced transient photocurrent measurement [69] and intensity modulated photocurrent spectroscopy [70] is more than two orders of magnitude smaller than the value for bulk anatase crystal [71]. This puzzling phenomenon is due to the network defects which results in trapping/detrapping of electrons within grain boundaries, and can be predicted using the “Multiple trapping” model [72]. Therefore, replacing TiO_2 nanoparticles with highly ordered nanostructure is expected to achieve a rapid electron transfer by minimizing the crystal trapping sites. Recently, it has been shown that the DSSCs based on the ordered arrays of TiO_2 or other metal oxide like ZnO manifest efficient charge separation and electron transfer feature.

Adachi et al. [71] reported a network structure of single-crystal-like TiO_2 nanowires formed through surfactant-assisted processes at a low temperature (353 K). The direction of crystal growth was controlled by changing the adsorption of surfactant molecules on the TiO_2 surface. A single-crystalline anatase exposing mainly the plane exhibits excellent ruthenium dye adsorption, four times higher as compared to commercial product P-25, thus leading to a high overall cell efficiency of 9.3%.

Law et al. [34] prepared zinc oxide (ZnO) nanowire arrays and first applied them to the DSSCs in 2005. ZnO nanowire arrays were formed according to the solution (ethanol) based process in which they adopted a modified seeded growth process to have a yield of long wires [73]. In their study, a 10–15 nm thick film of ZnO quantum dots was deposited onto FTO substrates by dip-coating. Nanowires grew from these nuclei through the thermal decomposition of a zinc complex. It is found the use of polyethylenimine (PEI), a cationic polyelectrolyte, has a striking effect as it hindered the lateral growth to increase the wire length. In this array, wire length and diameter varied from 16 to 17 μm and 130 to 200 nm, respectively. The prepared ZnO nanowire films are excellent conductors. The individual nanowire extracted from the arrays has a resistivity ranging from 0.3 to 2.0 Ω cm, with an electron concentration of $1–5 \times 10^{18}\ cm^{-3}$ and mobility of $1–5\ cm^2\ V^{-1}\ s^{-1}$. The electron diffusivity for single dry nanowire can be calculated from the Einstein relation:

$$D_n = \frac{k_B T \mu}{e} \tag{6}$$

where k_B is the Boltzmann constant, T is the absolute temperature, μ is the electron mobility, and e is the elementary charge. This value is several hundred times larger than the highest reported diffusivity for TiO_2 ($\approx 10^{-7}–10^{-4}\ cm^2\ s^{-1}$) and ZnO ($\approx 10^{-5}–10^{-3}\ cm^2\ s^{-1}$) nanoparticle films, which confirms that direct electrical pathways formed by the nanowires ensure rapid collection of carriers generated throughout the device. At a full Sun intensity of $100 \pm 3\ mW\ cm^{-2}$, the dye-sensitized solar cells with ZnO arrays were characterized by short-circuit density $J_{sc} = 5.3–5.85\ mA\ cm^{-2}$, $V_{oc} = 0.61–0.71\ V$, FF = 0.36–0.38, and overall conversion efficiency $\eta = 1.2–1.5\%$. The conversion efficiency is limited primarily by the surface area of the nanowire array, which only has one-fifth the active surface area of a nanoparticle anode.

Nanotubes with a hollow cavity structure offer a huge active surface area compared to that of nanowires. Attempts have been made to prepare such nanostructures. Adachi et al. [74] synthesized titania nanotubes by surfactant-assisted templating mechanism using molecular assemblies composed of surfactant molecules, i.e., laurylamine hydrochloride, titanium alkoxide, and tetraisopropylorthotitanate modified with acetylacetone, as a template. These nanotubes have outer and inner diameters of about 10 and 5 nm, respectively, and a length ranging from 30 nm to several hundred nanometers. The thin-film electrode made of titania nanotubes collected more than two times larger short-circuit current density than that of P-25 in the thin-film region, which explains the higher light to electricity conversion efficiency ($\approx 5\%$).

Because insufficient active surface area is a major limiting factor of nanotube application in DSSCs, it is of key interest to understand its dependence on the geometry parameter. To this end, both theoretical and experimental studies have been conducted recently. Assuming an idealized nanotubular structure as Fig. 8(a), the purely geometric roughness (physical surface area of the film per unit of projected area) is expressed as [75,76]

$$R_f = 1 + \frac{4\pi(D+W)}{\sqrt{3}(D+2W)^2} \tag{7}$$

where D is the inner diameter, W is the wall thickness, and L is the tube length. From the plot Fig. 8(b), it is shown that larger surface area is easily obtained by nanotubes with small porosity. Although each surface area of nanotubes is reduced according to the reduction in porosity, more nanotubes could be used to offset the individual loss to increase the total surface area (equivalent area).

Recently, Lei et al. [77] fabricated large-scale, noncurling anatase crystalline TiO_2 nanotube arrays on a FTO substrate via a four step process: (i) fabrication of TiO_2 nanotube on Ti foil by anodization, (ii) detachment of the amorphous free-standing TiO_2 nanotubes via ultrasonic treatment, (iii) transfer and adhesion to FTO substrates, and (iv) two-steps annealing treatment. For a 20.8 μm length array, an overall photoconversion efficiency of about 8.1% can be achieved.

4.4.3. Other novel morphology

Besides the nanowire and nanotube structure, many other highly ordered one-dimensional (1D) nanoarrays have been applied to dye-sensitized solar cells in recent years. A novel structure of submicrometer-sized mesopores TiO_2 beads was first reported by Chen et al. [78]. In their work, highly crystallized mesoporous TiO_2 beads with surface areas of up to $108\ m^2\ g^{-1}$ and tunable pore sizes (from 14.0 to 22.6 nm) have been prepared through a combined sol–gel and solvothermal process. This structure promotes light scattering on the electrodes, without sacrificing the accessible surface for dyes. An overall light conversion efficiency of 7.2% has been achieved by using these mesoporous TiO_2 beads as an electrode.

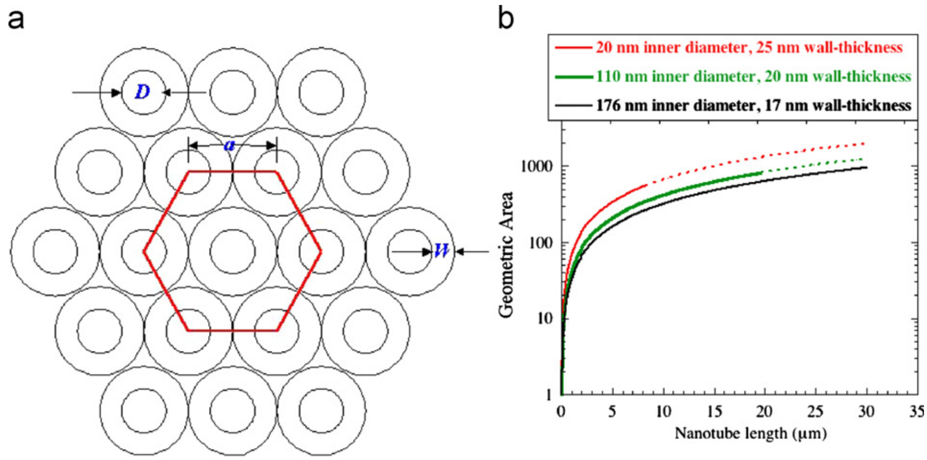


Fig. 8. (a) Idealized unit cell of TiO_2 nanotube array with inner diameter D, wall thickness W, and $a=D+W$ and (b) geometric roughness factor Vs nanotube length [76].

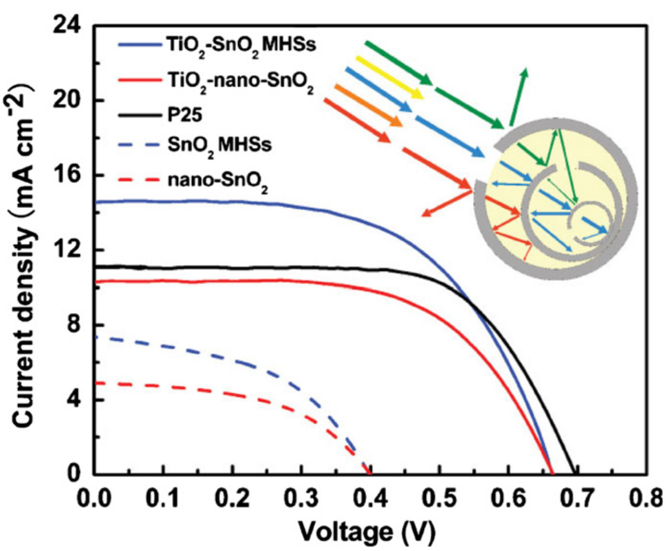


Fig. 9. J–V characteristics of DSSCs for different photoelectrode films [39]. (The inset illustrates the multiple reflecting and scattering of light in the multilayered hollow spheres.)

Yang et al. [79] first synthesized ordered hollow TiO_2 hemisphere films for photoelectrodes in DSSCs. They combined colloidal templates and rf-sputtering to deposit quasi-ordered hollow TiO_2 hemispheres onto conducting glass substrates with tunable hemisphere size and shell thickness. The hollow structure promotes electron transport and enhances dye loading by a large surface area. An enhanced photoconversion efficiency of 3.49% was achieved under air mass 1.5 illumination. Similar work has been conducted by Qian et al. [39]. They first synthesized TiO_2-coated multilayered SnO_2 hollow microspheres (MHSs, as shown in Fig. 9) by two steps. First, SnO_2 MHSs were prepared by a chemically induced self-assembly reaction of aqueous sucrose/$SnCl_4$ solution under a hydrothermal condition. The second step was to coat TiO_2 nanocrystallites onto the SnO_2 MHSs by impregnating in and then hydrolyzing $TiCl_4$ to form a surface layer of TiO_2. It was found that TiO_2-coated multilayered hollow SnO_2 microspheres exhibited a high photoconversion efficiency of 5.65%, a 34% improvement compared to the TiO_2-nano-SnO_2 film.

4.5. Theoretical study of charge transfer process

Much effort has been exerted to build models to simulate the working principle of dye-sensitized solar cells. Effective design of new device structure and its optimal performance is possible only by understanding the underlying mechanism. Sodergren et al. [80] presents a simple diffusion model of semiconductor films, which was based on two assumptions: (i) electron transport via diffusion only and (ii) the diffusion length is constant; i.e. recombination process is assumed to be of the first order. The governing equation used to describe electron transfer in semiconductor films can be expressed as

$$Dn''(x)-\frac{n(x)-n_0}{\tau}+\Phi\partial e^{-\partial x}=0 \tag{8}$$

where D is the diffusion constant of the electrons in the film, $n(x)$ is the excess electron density, n_0 is the electron density in the dark, Φ represents the incident light intensity, and α is the reciprocal absorption length. The solved I–V characteristic equation was similar to the expression for a p–n junction solar cell, but the properties of the electrolyte were not taken into account.

Later, Cao et al. [81] adopted this model to analyze the transient response of the cell and extended the diffusion coefficient as a function of the light intensity. However, the model only accounted for the production of electrons under illumination by a Beer–Lambert's law [82]. Papageorgiou et al. [83] investigated the electrolyte mass transport in thin layer nanocrystalline photoelectrochemical solar cells, and determined the concentration of the redox active species under steady state irradiation as a function of current density as well as location and direction of irradiation.

An improved simplified complete electrical model was presented by Ferber et al. [84] to evaluate the performance of DSSC by accounting the properties of the electrons in TiO_2 films as well as the charge transport in the electrolyte solution and redox processes at the counter electrode. The charge transport within the TiO_2 conduction band and the electrolyte system was described with continuity and mass transport equations, and the macroscopic electric field was calculated using Poisson's equation. Although more details are included in the model, the interfacial model of the semiconductor/dye/electrolyte interface does not include all reactions. The electron transport dynamics have been modeled using simulated mesoporous random nanoparticle TiO_2 films and the random-walk approach [67]. Diffusion (random walk) in such networks was described in terms of the percolation theory, which predicted the power-law dependence (exponent μ) of the diffusion coefficient on the difference between the film porosity (P) and some critical porosity (P_c): $D\propto|P-P_c|^{\mu}$.

5. Electrolyte development

The electrolyte is a key component of all dye-sensitized solar cells (DSSCs). It functions as charge carriers collecting electrons at

the cathode and transporting the electrons back to the dye molecule. In terms of the cell efficiency, the most popularly used electrolyte is the iodide/triiodide (I^-/I_3^-) redox couple in an organic matrix, generally acetonitrile. However, there exist undesirable intrinsic properties which are inherent of a liquid electrolyte significantly affecting a device's long-term durability and operational stability. For example, not only the leakage of toxic organic solvent will cause environmental contamination, but also the evaporation of volatile iodine ions will increase the overall internal resistance by lowering concentration of the charge carrier. To overcome these disadvantages, research has been conducted to develop non-traditional electrolytes e.g. room temperature ionic liquids (RTILs), quasi-solid state and solid state electrolytes.

5.1. Liquid electrolyte

The most commonly used liquid electrolyte, namely iodide/triiodide (I^-/I_3^-), works well mainly due to its kinetics as shown in Fig. 10 [85]. The electron injection into the TiO_2 conduction band occurs in the femtosecond time range which is much faster than the electron recombination with I_3^-, and the oxidized dye preferably reacts with I^- than combining with the injected electrons. In the electrolyte, the I_3^- diffuses to cathode to harvest electrons and in turn produce I^- which diffuses in the opposite direction towards the TiO_2 electrode to regenerated dye molecules. The diffusion coefficient of I_3^- ions in the porous TiO_2 structure is about $7.6 \times 10^{-6}\ cm^2/s$ [62].

One important issue to be considered when using the I^-/I_3^- redox couple is its concentration. At low iodine concentration, it is difficult to maintain sufficient electrolyte conductivity and rapid redox reaction. On the other hand, when iodine concentration is high, electron recombination at the TiO_2 interface deteriorates the performance of DSSCs and meanwhile the rate of light absorption by redox couple is increased [86]. The exact quantitative relationship is expressed in Eq. (3) which shows that electron recombination process determines the open circuit voltage (V_{oc}) which depends on the concentration of triiodide in the TiO_2.

It is found that recombination can be suppressed by introducing additives to the electrolyte such as 4-tert-butylpyridine (4TBP) [87], guanidiumthiocyanate [88], and methylbenzimidazole (MBI) [89]. These additives can improve the efficiency and stability, though they do not participate in the fundamental photoelectrochemical processes. The most probable mechanism is that these additives when absorbed by the TiO_2 surface block the reduction sites to keep electron acceptor molecules away from contact. A similar phenomenon was observed by Zhang et al. [90] when adding co-adsorbents in a dye bath.

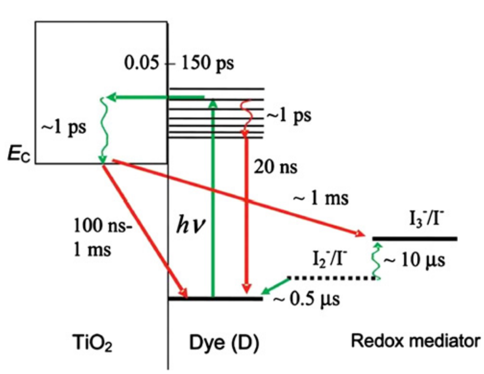


Fig. 10. Kinetics of the *cis*-Ru(dcbpy)$_2$(NCS)$_2$-sensitized TiO_2 solar cell with I^-/I_3^- redox mediator [85].

In theory, the maximum voltage generated in DSSCs is determined by the difference between the quasi-Fermi level of the TiO_2 and the redox potential of the electrolyte, about 0.7 V under solar illumination conditions. In order to obtain a higher open circuit voltage and circumvent the corrosion of I^-/I_3^- redox couple, a variety of alternative redox couples have been introduced to DSSCs such as Br^-/Br_3^-, $SCN^-/(SCN)_2$, $SeCN^-/(SeCN)_3^-$, $Fe(CN)_6^{3-/4-}$ [91] and Co(II)/Co(III) complex. Recently, Wang et al. [92] reported a new disulfide/thiolate redox couple that has negligible absorption in the visible spectral range and achieved an unprecedented efficiency of 6.4% under standard illumination test conditions. This novel redox couple set a new benchmark for iodide-free DSSCs by offering a viable pathway to scale up and practical applications. The best alternative redox couple to date seems to be cobalt polypyridine complexes, because of their weak visible light absorption, the higher redox potential and the less aggressive corrosiveness towards metallic conductors. Recent research [29,93,94] has proven that by tuning their redox potential to match the oxidation potential of the sensitizer can minimize the energy loss in the dye regeneration step and leads to attainment of strikingly high open-circuit voltage approaching 1 V.

Other than redox couple electrolyte, a new type of liquid electrolyte, i.e. room temperature ionic liquids (RTILs), has shown promising potential to serve as an alternative electrolyte. RTILs are a group of organic salts containing cations such as imidazolium, pyridinium and anions from the halide or pseudo-halid family [95]. Because of these structures, they function simultaneously as iodide source and as solvent [96]. It is expected that RTILs could solve the sealing problem and enhance the stability by virtue of their inherent characteristics like good chemical and thermal stability, negligible vapor pressure, non-flammability, and high ionic conductivity.

The first application of RTIL to DSSCs was reported by Papageorgiou et al. [97]. In their study methyl-hexyl-imidazolium iodide (MHImI) was added as an iodide resource which was found to be the least viscous iodide molten at room temperature and not sensitive to water moisture. Outstanding stability was achieved with an estimated sensitizer turnover in excess of 50 million times. However, the photovoltaic performance was very low due to low iodide concentration, as well as its viscosity being relatively high (1800 cP at 25 °C) compared to the water (0.890 cP). Research continues on the application of RTIL, and many other molten salts, such as 1,3-dialkylimidazolium, 1,2,3-trialkylimidazolium, and *N*-alkylpyridinium [98], have been tested with DSSCs for their compatibility. The current milestone for ionic electrolyte development is that eutectic salts have been used to achieve a remarkable efficiency of 8.2% [99].

5.2. Solid-state electrolyte

A solid-sate electrolyte is considered to be an alternative to the liquid electrolyte, because it could achieve a better mechanical stability and simplified fabrication processes. It is an essentially simple idea that replaces the liquid electrolyte with inorganic p-type semiconductors or organic hole transporting materials to eliminate the evaporation and leakage of liquid electrolyte. In this sense, the n-type semiconductor and p-type sensitizer make dye-sensitized solar cells inevitably analogous with traditional Si-based p–n junction solar cells in principle. A suitable hole-transport material must have a band gap structure compatible with the highest occupied molecular orbital (HOMO) level of the dye and the conduction band of TiO_2 to drive the charge-transfer process. The main difficulty in realizing such a solid-state electrolyte device is to form an intimate contact at the p–n junction interfaces.

The first p-type semiconductors acting as hole-transport materials were CuSCN and CuI, introduced by Tennakone et al. [100] and O'Regan and Schwartz [101]. In their first step, they could achieve an overall efficiency less than 1%, due to the formation of unfilled voids in the TiO_2 intercrystallite. During the deposition process, p-CuI crystalline semiconductors experience a rapid crystal growth. The formation of a crystal with a dimension exceeding that of TiO_2 pores will interfere with the filling process, leaving a large portion of pores unfilled. Later Kumara et al. [102] found an effective crystal growth inhibitor triethylaminehydrothiocyannate (THT) to improve the cell efficiency to 3.75%. Recently, a novel working electrode TiO_2/CuI/Cu was reported by Heng et al. [103]. In their study, the CuI layer was deposited on a copper mesh to form a p–n junction with TiO_2. This structure forms a single directional pathway for efficient electron transport, which led to a high conversion efficiency of up to 4.73% under 1 sun illumination. As for p-type organic semiconductors, spiro-OMeTAD has proven to be the most successful one. It was initially presented by Bach et al. [104] in 1998, and since then the conversion yield of its device has been increasing and has reached about 4%.

5.3. Quasi-solid electrolyte

As mentioned in the last two sections, most of the works have reported that the conversion efficiency of DSSCs using solid electrolyte is lower, typically less than 5%. This is due to the fact of poor contact at TiO_2/electrolyte interface and conductivity of these materials is generally low [105]. In order to circumvent the above drawbacks, an alternative solution is proposed and attempted where both liquid and solid electrolytes can be combined to form a quasi-solid electrolyte, or gel electrolyte. Apparently, there are several advantages of using gel electrolyte: (i) relatively high ambient ionic conductivity (6–8 mS cm^{-1}), (ii) intimate interfacial contact with TiO_2, and (iii) remarkable electrolyte stability. At the initial step, the solvent with a low viscosity penetrates the TiO_2 mesopores to form a good contact. After gelation volatile liquid solvent is encapsulated within a gel network that prevents the electrolyte evaporation and leakage.

Wang et al. [106] demonstrated that PVDF-HFP polymer can confine MPN-based liquid electrolyte into gel without hampering charge transport of the triiodide/iodide couple inside the polymer network. A conversion yield higher than 6% was obtained. In addition, the cell with such gel electrolyte sustained heating for 1000 h at 80 °C, maintaining 94% of its initial performance. Later, the ionic liquid was seminally solidified by adding silica nanoparticles to produce an ionic liquid-based quasi-solid state electrolyte which achieved an efficiency of 7% [107].

6. Future prospectus

Dye sensitized-solar cell (DSSC) has proven its potential as a cheap alternative to expensive silicon solar cells. It is a cost-effective technology that features relatively high efficiency, long-term stability and easy fabrication. In addition, DSSCs are more sensitive than crystalline silicon cells to visible light, and light incident at a shallow angle. Such characteristics enable DSSCs to be a reliable power source in low light intensity environment. Currently, DSSCs are still under laboratory research and development stage. Much work remains to be conducted to further improve its energy conversion efficiency for practical applications.

Dyes, as a key component of DSSCs, have been receiving intensive research attention, because the light-to-electrical conversion of DSSCs strongly depends on the light absorption of sensitized dyes. Comprehensive studies aiming at synthesizing panchromatic dyes have been conducted for decades. However, as a general rule, dyes that absorb strongly do not typically exhibit broad absorption. Recently, Hardin et al. [108] presented a new design where high-energy photons are absorbed by highly photoluminescent chromosphores unattached to the titania and undergo Förster resonant energy transfer to the sensitizing dye. Different from co-sensitized technology, this novel architecture offers an alternative pathway to increase light harvesting in DSSCs.

Besides enhancing the performance, how to lower materials cost is another important issue that needs to be addressed in the future work. Wang and Kerr [109] attempted to use paper as substrate to make flexible DSSCs (efficiency 2.66%). Although the Ni coated paper substrate is prone to crack generated in calcinations, the mature coating technology of paper substrate can provide an opportunity for low cost roll to roll mass production. The expensive metal platinum is used as electrocatalyst on the cathode in DSSCs, and the necessary amount of platinum is ca. 10–100 $\mu g/cm^2$. In order to lower the materials' cost and obtain a good optical transparency, various noble metal-free materials are prepared and tested to examine their compatibility in DSSCs. Recently, Wang et al. [110] reported that CoS (cobalt sulfide) nanoparticles deposited electronchemically on the flexible ITO/PEN film, match the performance of Pt as a triiodide reduction catalyst in DSSCs. Remarkably, the cost of cobalt is several hundred times lower than that of platinum. Kavan et al. [111] fabricated semitransparent (> 85%) thin films on F-doped SnO_2 (FTO) using commercial grapheme nanoplatelets. Such graphene cathode exhibits comparable performance with the Pt cathode in ionic liquid based DSSCs. Moreover, this optical transparency is an essential feature that extends certain applications to tandem cells, windows and roof panels.

Apart from improving the performance of single component in DSSCs, tandem pn-DSSC is another option for further endeavors. Tandem cells combining the p-type DSSCs with typical n-type DSSCs could achieve a much better efficiency than single-junction DSSC, because it can harvest natural light more effectively by using spectral complementary dyes. Recently, Nattestad et al. [112] designed a series of donor–acceptor dyes which comprise a variable-length oligothiophene bridge to control over the spatial separation of photogenerated charge carriers. It was found that such dyes significantly decelerated charge recombination in p-type DSSC and achieved an absorbed photon to electrons efficiency up to 96%. Tandem cells assembled with such p-type DSSCs exceeded the efficiency of their individual components. If a spectral complement of dyes and energy band structure of semiconductors can be effectively optimized in the near future,

Table 1
The highest efficiency achieved based on the different semiconductor materials.

Process	Composition	μ_H ($cm^2 V^{-1} s^{-1}$)	V_{oc} (V)	J_{sc} (mA cm^{-2})	FF	η (%)
Hydrothermal	Zn_2SnO_4		0.62	9.3	0.66	3.8 [47]
Squeegee method	ZnO		0.62	18.11	0.59	6.6 [38]
Surface spray	MgO/SnO_2	100–200	0.75	14.21	0.67	7.2 [46]
Screen-printing	TiO_2	0.1–1	0.74	20.9	0.72	11.1 [25]

tandem cells will gain momentum in cell efficiency as well as processing and materials cost, because the only change of tandem cells is to replace the expensive catalytic platinum layer with a dye-sensitized p-type semiconductor layer.

The start of market exploration is key to future prosperity of DSSCs. Companies such as Sony, Konarka, and G24 Innovations have launched a campaign to facilitate DSSCs' commercial availability. Recently, Sony [113] developed its own unique approach, known as the 'Concerto Effect'. In August 2010, efficiency was further enhanced to 9.9% using black dye and D131. The combined performance of the two dyes was greater than the sum of their individual performance levels.

7. Conclusion

As a novel photovoltaic technology, dye-sensitized solar cells (DSSCs) have potential to compete with traditional solar cells. Materials such as TiO_2 used in DSSCs are generally inexpensive, abundant and innocuous to the environment. Compared with silicon solar cells, they are insensitive to impurities in fabrication process, which accelerates a transition from research laboratory to mass production line. From the perspective of application, low weight and flexibility of DSSCs are desirable for the portable electronic device. It is found that DSSCs work better than silicon solar cells in the darker condition, for example, in the dawn and dusk, and also the overall efficiency is not seriously affected in the high temperature. In addition, the transparency and varied color of DSSCs could be utilized for decorative purposes like windows and sunroof. Up to now, such benefits have attracted considerable company investment and government funding. It is believed that with consistent efforts, DSSCs will be a reliable electrical power supplier in the future (Table 1).

References

[1] 〈http://www.energy.eu/〉.
[2] 〈http://www.whitehouse.gov/issues/energy-and-environment〉.
[3] Nobuyuki H. Renewable energy: RD&D priorities: insights from IEA technology programmes; 2006.
[4] REN21. Renewables 2010 Global Status Report.
[5] Hasan MA, Sumathy K. Photovoltaic thermal module concepts and their performance analysis: a review. Renewable and Sustainable Energy Reviews 2010;14(7):1845–59.
[6] Hoppe H, Sariciftci NS. Organic solar cells: an overview. Journal of Materials Research 2004;19(7):1924–45.
[7] Gunes S, Neugebauer H, Sariciftci NS. Conjugated polymer-based organic solar cells. Chemical Reviews 2007;107(4):1324–38.
[8] O'regan B, Grätzel M. A low-cost, high-efficiency solar cell based on dye-sensitized colloidal TiO_2 films. nature 1991;353(6346):737–40.
[9] Gao F, Wang Y, Shi D, Zhang J, Wang M, Jing X, et al. Enhance the optical absorptivity of nanocrystalline TiO_2 film with high molar extinction coefficient ruthenium sensitizers for high performance dye-sensitized solar cells. Journal of the American Chemical Society 2008;130(32):10720–8.
[10] 〈http://en.wikipedia.org/wiki/Dye-sensitized_solar_cell#cite_note-30〉.
[11] Sima C, Grigoriu C, Antohe S. Comparison of the dye-sensitized solar cells performances based on transparent conductive ITO and FTO. Thin Solid Films 2010;519(2):595–7.
[12] Hagfeldt A, Grätzel M. Molecular photovoltaics. Accounts of Chemical Research 2000;33(5):269–77.
[13] O'Regan B, Lenzmann F, Muis R, Wienke J. A solid-state dye-sensitized solar cell fabricated with pressure-treated P25-TiO_2 and CuSCN: Analysis of pore filling and IV characteristics. Chemistry of Materials 2002;14(12):5023–9.
[14] Taguchi T, Zhang XT, Sutanto I, Tokuhiro K, Rao TN, Watanabe H, Nakamori T, Uragami M, Fujishima A. Improving the performance of solid-state dye-sensitized solar cell using MgO-coated TiO_2 nanoporous film. Chemical Communications 2003;19:2480–1.
[15] Murakoshi K, Kogure R, Wada Y, Yanagida S. Fabrication of solid-state dye-sensitized TiO_2 solar cells combined with polypyrrole. Solar Energy Materials and Solar Cells 1998;55(1):113–25.
[16] Hagen J, Schaffrath W, Otschik P, Fink R, Bacher A, Schmidt HW, Haarer D. Novel hybrid solar cells consisting of inorganic nanoparticles and an organic hole transport material. Synthetic metals 1997;89(3):215–20.
[17] Arango AC, Johnson LR, Bliznyuk VN, Schlesinger Z, Carter SA, Hörhold HH. Efficient titanium oxide/conjugated polymer photovoltaics for solar energy conversion. Advanced Materials 2000;12(22):1689–92.
[18] Calandra P, Calogero G, Sinopoli A, Gucciardi PG. Metal nanoparticles and carbon-based nanostructures as advanced materials for cathode application in dye-sensitized solar cells. Catalyst 2010;3:4a.
[19] Lan Z, Wu J, Wang D, Hao S, Lin J, Huang Y. Quasi-solid-state dye-sensitized solar cells based on a sol–gel organic–inorganic composite electrolyte containing an organic iodide salt. Solar Energy 2007;81(1): 117–122.
[20] Han L, Koide N, Chiba Y, Islam A, Mitate T. Modeling of an equivalent circuit for dye-sensitized solar cells. Applied Physics Letters 2004;84(13):2433–5.
[21] Wang Q, Moser JE, Grätzel M. Electrochemical impedance spectroscopic analysis of dye-sensitized solar cells. Journal of Physical Chemistry B 2005;109(31):14945–53.
[22] Nazeeruddin MK, Kay A, Rodicio I, Humphry-Baker R, Mueller E, Liska P, Vlachopoulos N, Graetzel M. Conversion of light to electricity by cis-X2bis (2,2′-bipyridyl-4,4′-dicarboxylate) ruthenium (II) charge-transfer sensitizers (X= Cl–, Br–, I–, CN–, and SCN–) on nanocrystalline titanium dioxide electrodes. Journal of the American Chemical Society 1993;115(14): 6382–6390.
[23] Nazeeruddin MK, Pechy P, Grätzel M. Efficient panchromatic sensitization of nanocrystallineTiO_2 films by a black dye based on atrithiocyanato-ruthenium complex. Chemical Communications 1997;18:1705–6.
[24] Nazeeruddin MK, Péchy P, Renouard T, Zakeeruddin SM, Humphry-Baker R, Comte P, Liska P, Cevey L, Costa E, Shklover V, Spiccia L, Deacon GB, Bignozzi CA, Grätzel M. Engineering of efficient panchromatic sensitizers for nanocrystalline TiO_2-based solar cells. Journal of the American Chemical Society 2001;123(8):1613–24.
[25] Chiba Y, Islam A, Watanabe Y, Komiya R, Koide N, Han L. Dye-sensitized solar cells with conversion efficiency of 11.1%. Japanese Journal of Applied Physics Part 2-Letters & Express Letters 2006;45(24–28):L638–40.
[26] Grätzel M. Recent advances in sensitized mesoscopic solar cells. Accounts of Chemical Research 2009;42(11):1788–98.
[27] Mishra A, Fischer MKR, Bauerle P. Metal-free organic dyes for dye-sensitized solar cells: from structure: property relationships to design rules. Angewandte Chemie—International Edition 2009;48(14):2474–99.
[28] Hwang S, Lee JH, Park C, Lee H, Kim C, Park C, Lee MH, Lee W, Park J, Kim K, Park NG, Kim C. A highly efficient organic sensitizer for dye-sensitized solar cells. Chemical Communications 2007;46:4887–9.
[29] Yella A, Lee HW, Tsao HN, Yi C, Chandiran AK, Nazeeruddin MK, Diau EWG, Yeh CY, Zakeeruddin SM, Grätzel M. Porphyrin-sensitized solar cells with cobalt (II/III)-based redox electrolyte exceed 12 percent efficiency. Science 2011;334(6056):629–34.
[30] Zhou H, Wu L, Gao Y, Ma T. Dye-sensitized solar cells using 20 natural dyes as sensitizers. Journal of Photochemistry and Photobiology A—Chemistry 2011;219(2-3):188–94.
[31] Wang ZS, Cui Y, Dan-oh Y, Kasada C, Shinpo A, Hara K. Molecular design of coumarin dyes for stable and efficient organic dye-sensitized solar cells. Journal of Physical Chemistry C 2008;112(43):17011–7.
[32] Hoffmann MR, Martin ST, Choi W, Bahnemann DW. Environmental applications of semiconductor photocatalysis. Chemical Reviews 1995;95(1): 69–96.
[33] Park NG, van de Lagemaat J, Frank AJ. Comparison of dye-sensitized rutile- and anatase-based TiO_2 solar cells. Journal of Physical Chemistry B 2000;104(38):8989–94.
[34] Law M, Greene LE, Johnson JC, Saykally R, Yang P. Nanowire dye-sensitized solar cells. Nature Materials 2005;4(6):455–9.
[35] Redmond G, Fitzmaurice D, Graetzel M. Visible light sensitization by cis–bis (thiocyanato) bis (2,2′-bipyridyl-4,4′-dicarboxylato) ruthenium (II) of a transparent nanocrystalline ZnO film prepared by sol–gel techniques. Chemistry of Materials 1994;6(5):686–91.
[36] Keis K, Magnusson E, Lindström H, Lindquist SE, Hagfeldt A. A 5% efficient photoelectrochemical solar cell based on nanostructured ZnO electrodes. Solar Energy Materials and Solar Cells 2002;73(1):51–8.
[37] Jose R, Thavasi V, Ramakrishna. S. Metal oxides for dye-sensitized solar cells. Journal of the American Ceramic Society 2009;92(2):289–301.
[38] Saito M, Fujihara S. Large photocurrent generation in dye-sensitized ZnO solar cells. Energy and Environmental Science 2008;1(2):280–3.
[39] Qian J, Liu P, Xiao Y, Jiang Y, Cao Y, Ai X, Yang H. TiO_2-Coated Multilayered SnO_2 Hollow Microspheres for dye-sensitized solar cells. Advanced Materials 2009;21(36):3663–7.
[40] Fonstad C, Rediker R. Electrical properties of high-quality stannic oxide crystals. Journal of Applied Physics 1971;42(7):2911–8.
[41] Breckenridge RG, Hosler WR. Electrical properties of titanium dioxide semiconductors. Physical Review 1953;91(4):793–802.
[42] Ramasamy E, Lee. J. Ordered mesoporous SnO_2-based photoanodes for high-performance dye-sensitized solar cells. Journal of Physical Chemistry C 2010;114(50):22032–7.
[43] Fukai Y, Kondo Y, Mori S, Suzuki E. Highly efficient dye-sensitized SnO_2 solar cells having sufficient electron diffusion length. Electrochemistry Communications 2007;9(7):1439–43.
[44] Green ANM, Palomares E, Haque SA, Kroon JM, Durrant JR. Charge transport versus recombination in dye-sensitized solar cells employing nanocrystalline TiO_2 and SnO_2 films. Journal of Physical Chemistry B 2005;109(25):12525–33.

[45] Parks GA. The isoelectric points of solid oxides, solid hydroxides, and aqueous hydroxo complex systems. Chemical Reviews 1965;65(2):177–98.
[46] Senevirathna MKI, Pitigala PKDDP, Premalal EVA, Tennakone K, Kumara GRA, Konno A. Stability of the SnO_2/MgO dye-sensitized photoelectrochemical solar cell. Solar Energy Materials and Solar Cells 2007;91(6):544–7.
[47] Tan B, Toman E, Li Y, Wu Y. Zinc stannate (Zn_2SnO_4) dye-sensitized solar cells. Journal of the American Chemical Society 2007;129(14):4162–3.
[48] Huang L, Jiang L, Wei. M. Metal-free indoline dye sensitized solar cells based on nanocrystalline Zn_2SnO_4. Electrochemistry Communications 2010;12(2): 319–22.
[49] Tahar RBH, Ban T, Ohya Y, Takahashi Y. Tin doped indium oxide thin films: electrical properties. Journal of Applied Physics 1998;83(5):2631–45.
[50] Hamberg I, Granqvist CG. Evaporated Sn-doped In_2O_3 films: basic optical properties and applications to energy-efficient windows. Journal of Applied Physics 1986;60(11):R123–60.
[51] Ngamsinlapasathian S, Sreethawong T, Suzuki Y, Yoshikawa S. Doubled layered ITO/SnO_2 conducting glass for substrate of dye-sensitized solar cells. Solar Energy Materials and Solar Cells 2006;90(14):2129–40.
[52] Ngamsinlapasathian S, Sreethawong T, Yoshikawa S. Enhanced efficiency of dye-sensitized solar cell using double-layered conducting glass. Thin Solid Films 2008;516(21):7802–6.
[53] Yang F. Thin film solar cells grown by organic vapor phase deposition. Princeton University; 2009.
[54] Chen Z, Cotterell B, Wang W, Guenther E, Chua SJ. A mechanical assessment of flexible optoelectronic devices. Thin Solid Films 2001;394(1):201–5.
[55] Wang X, Zhi L, Müllen K. Transparent, conductive graphene electrodes for dye-sensitized solar cells. Nano Letters 2008;8(1):323–7.
[56] Zhu H, Wei J, Wang K, Wu D. Applications of carbon materials in photovoltaic solar cells. Solar Energy Materials and Solar Cells 2009;93(9):1461–70.
[57] Hagfeldt A, Graetzel M. Light-induced redox reactions in nanocrystalline systems. Chemical Reviews (United States) 1995;95:1.
[58] Rühle S, Cahen D. Electron tunneling at the TiO_2/substrate interface can determine dye-sensitized solar cell performance. Journal of Physical Chemistry B 2004;108(46):17946–51.
[59] Asbury JB, Hao E, Wang Y, Ghosh HN, Lian T. Ultrafast electron transfer dynamics from molecular adsorbates to semiconductor nanocrystalline thin films. Journal of Physical Chemistry B 2001;105(20):4545–57.
[60] Yu H, Zhang S, Zhao H, Will G, Liu P. An efficient and low-cost TiO_2 compact layer for performance improvement of dye-sensitized solar cells. Electrochimica Acta 2009;54(4):1319–24.
[61] Cameron PJ, Peter LM. Characterization of titanium dioxide blocking layers in dye-sensitized nanocrystalline solar cells. Journal of Physical Chemistry B 2003;107(51):14394–400.
[62] Huang SY, Schlichthörl G, Nozik AJ, Grätzel M, Frank AJ. Charge recombination in dye-sensitized nanocrystalline TiO_2 solar cells. Journal of Physical Chemistry B 1997;101(14):2576–82.
[63] Grätzel M. Dye-sensitized solar cells. Journal of Photochemistry and Photobiology C: Photochemistry Reviews 2003;4(2):145–53.
[64] Sato S, Oimatsu S, Takahashi R. Pore size regulation of TiO_2 by use of a complex of titanium tetraisopropoxide and stearic acid. Chemical Communications 1997;22:2219–20.
[65] Barbé CJ, Arendse F, Comte P, Jirousek M, Lenzmann F, Shklover V, Grätzel M. Nanocrystalline titanium oxide electrodes for photovoltaic applications. Journal of the American Ceramic Society 1997;80(12):3157–71.
[66] Saito Y, Kambe S, Kitamura T, Wada Y, Yanagida S. Morphology control of mesoporous TiO_2 nanocrystalline films for performance of dye-sensitized solar cells. Solar Energy Materials and Solar Cells 2004;83(1):1–13.
[67] Benkstein KD, Kopidakis N, van de Lagemaat J, Frank AJ. Influence of the percolation network geometry on electron transport in dye-sensitized titanium dioxide solar cells. Journal of Physical Chemistry B 2003;107(31):7759–67.
[68] Wang ZS, Kawauchi H, Kashima T, Arakawa H. Significant influence of TiO_2 photoelectrode morphology on the energy conversion efficiency of N719 dye-sensitized solar cell. Coordination Chemistry Reviews 2004;248(13): 1381–1389.
[69] Solbrand A, Lindström H, Rensmo H, Hagfeldt A, Lindquist SE, Solbrand A, et al. Electron transport in the nanostructured TiO_2-electrolyte system studied with time-resolved photocurrents. Journal of Physical Chemistry B 1997;101(14):2514–8.
[70] Fisher AC, Peter LM, Ponomarev EA, Walker AB, Wijayantha KGU. Intensity dependence of the back reaction and transport of electrons in dye-sensitized nanocrystalline TiO_2 solar cells. Journal of Physical Chemistry B 2000;104(5):949–58.
[71] Adachi M, Murata Y, Takao J, Jiu J, Sakamoto M, Wang F. Highly efficient dye-sensitized solar cells with a titania thin-film electrode composed of a network structure of single-crystal-like TiO_2 nanowires made by the "oriented attachment" mechanism. Journal of the American Chemical Society 2004;126(45):14943–9.
[72] Frank AJ, Kopidakis N, Lagemaat J. Electrons in nanostructured TiO_2 solar cells: transport, recombination and photovoltaic properties. Coordination Chemistry Reviews 2004;248(13):1165–79.
[73] Greene LE, Law M, Goldberger J, Kim F, Johnson JC, Zhang Y, Saykally RJ, Yang P. Low-temperature wafer-scale production of ZnO nanowire arrays. Angewandte Chemie International Edition 2003;42(26):3031–4.
[74] Adachi M, Murata Y, Okada I, Yoshikawa S. Formation of titania nanotubes and applications for dye-sensitized solar cells. Journal of the Electrochemical Society 2003;150:G488–93.
[75] Shankar K, Basham JI, Allam NK, Varghese OK, Mor GK, Feng X, Paulose M, Seabold JA, Choi KS, Grimes CA. Recent advances in the use of TiO_2 nanotube and nanowire arrays for oxidative photoelectrochemistry. Journal of Physical Chemistry C 2009;113(16):6327–59.
[76] Shankar K, Mor GK, Prakasam HE, Yoriya S, Paulose M, Varghese OK, Grimes CA. Highly-ordered TiO_2 nanotube arrays up to 220 μm in length: use in water photoelectrolysis and dye-sensitized solar cells. Nanotechnology 2007;18(6):065707.
[77] Lei BX, Liao JY, Zhang R, Wang J, Su CY, Kuang DB. Ordered crystalline TiO_2 nanotube arrays on transparent FTO glass for efficient dye-sensitized solar cells. Journal of Physical Chemistry C 2010;114(35):15228–33.
[78] Chen D, Huang F, Cheng YB, Caruso RA. Mesoporous anatase TiO_2 Beads with high surface areas and controllable pore sizes: a superior candidate for high-performance dye-sensitized solar cells. Advanced Materials 2009;21(21):2206–10.
[79] Yang SC, Yang DJ, Kim J, Hong JM, Kim HG, Kim ID, Lee H. Hollow TiO_2 hemispheres obtained by colloidal templating for application in dye-sensitized solar cells. Advanced Materials 2008;20(5):1059–64.
[80] Soedergren S, Hagfeldt A, Olsson J, Lindquist SE. Theoretical models for the action spectrum and the current–voltage characteristics of microporous semiconductor films in photoelectrochemical cells. Journal of Physical Chemistry 1994;98(21):5552–6.
[81] Cao F, Oskam G, Meyer GJ, Searson PC. Electron transport in porous nanocrystalline TiO_2 photoelectrochemical cells. Journal of Physical Chemistry 1996;100(42):17021–7.
[82] Penny M, Farrell T, Will. G. A mathematical model for the anodic half cell of a dye-sensitised solar cell. Solar Energy Materials and Solar Cells 2008;92(1):24–37.
[83] Papageorgiou N, Grätzel M, Infelta P. On the relevance of mass transport in thin layer nanocrystalline photoelectrochemical solar cells. Solar Energy Materials and Solar Cells 1996;44(4):405–38.
[84] Ferber J, Stangl R, Luther J. An electrical model of the dye-sensitized solar cell. Solar Energy Materials and Solar Cells 1998;53(1):29–54.
[85] Boschloo G, Hagfeldt A. Characteristics of the iodide/triiodide redox mediator in dye-sensitized solar cells. Accounts of Chemical Research 2009;42(11):1819–26.
[86] Zanni MT, Greenblatt BJ, Davis AV, Neumark DM. Photodissociation of gas phase I using femtosecond photoelectron spectroscopy. Journal of Chemical Physics 1999;111(7):2991.
[87] Boschloo G, Häggman L, Hagfeldt A. Quantification of the effect of 4-tert-butylpyridine addition to I^-/I_3^- redox electrolytes in dye-sensitized nanostructured TiO_2 solar cells. Journal of Physical Chemistry B 2006;110(26): 13144–50.
[88] Kopidakis N, Neale NR, Frank AJ. Effect of an adsorbent on recombination and band-edge movement in dye-sensitized TiO_2 solar cells: evidence for surface passivation. Journal of Physical Chemistry B 2006;110(25): 12485–9.
[89] Figgemeier E, Hagfeldt A. Are dye-sensitized nano-structured solar cells stable? An overview of device testing and component analyses International Journal of Photoenergy 2004;6(3):127–40.
[90] Zhang Z, Evans N, Zakeeruddin SM, Humphry-Baker R, Grätzel M. Effects of ω-guanidinoalkyl acids as coadsorbents in dye-sensitized solar cells. Journal of Physical Chemistry C 2007;111(1):398–403.
[91] Daeneke T, Uemura Y, Duffy NW, Mozer AJ, Koumura N, Bach U, Spiccia L. Aqueous dye-sensitized solar cell electrolytes based on the ferricyanide-ferrocyanide redox couple. Advanced Materials, 2012.
[92] Wang M, Chamberland N, Breau L, Moser JE, Humphry-Baker R, Marsan B, Zakeeruddin SM, Grätzel M. An organic redox electrolyte to rival triiodide/iodide in dye-sensitized solar cells. Nature Chemistry 2010;2(5):385–9.
[93] Feldt SM, Gibson EA, Gabrielsson E, Sun L, Boschloo G, Hagfeldt A. Design of organic dyes and cobalt polypyridine redox mediators for high-efficiency dye-sensitized solar cells. Journal of the American Chemical Society 2010;132(46):16714–24.
[94] Yum JH, Baranoff E, Kessler F, Moehl T, Ahmad S, Bessho T, Marchioro A, Ghadiri E, Moser JE, Yi C, Nazeeruddin MK, Grätzel M. A cobalt complex redox shuttle for dye-sensitized solar cells with high open-circuit potentials. Nature Communications 2012;3:631.
[95] Zakeeruddin SM, Grätzel. M. Solvent-free ionic liquid electrolytes for mesoscopic dye-sensitized solar cells. Advanced Functional Materials 2009;19(14):2187–202.
[96] Gonçalves LM, Bermudez V, Ribeiro VZ, Mendes HA. AM. Dye-sensitized solar cells: a safe bet for the future. Energy & Environmetal Science 2008;1(6):655–67.
[97] Papageorgiou N, Athanassov Y, Armand M, Bonhote P, Pettersson H, Azam A, Graetzel M. The performance and stability of ambient temperature molten salts for solar cell applications. Journal of the Electrochemical Society 1996;143(10):3099–108.
[98] Gorlov M, Pettersson H, Hagfeldt A, Kloo L. Electrolytes for dye-sensitized solar cells based on interhalogen ionic salts and liquids. Inorganic Chemistry 2007;46(9):3566–75.
[99] Bai Y, Cao Y, Zhang J, Wang M, Li R, Wang P, Zakeeruddin SM, Grätzel M. High-performance dye-sensitized solar cells based on solvent-free electrolytes produced from eutectic melts. Nature Materials 2008;7(8):626–30.

[100] Tennakone K, Kumara GRRA, Kumarasinghe AR, Wijayantha KGU, Sirimanne PM. A dye-sensitized nano-porous solid-state photovoltaic cell. Semiconductor Science and Technology 1995;10(12):1689–93.
[101] O'Regan B, Schwartz DT. Efficient photo-hole injection from adsorbed cyanine dyes into electrodeposited copper (I) thiocyanate thin films. Chemistry of Materials 1995;7(7):1349–54.
[102] Kumara GRA, Kaneko S, Okuya M, Tennakone K. Fabrication of dye-sensitized solar cells using triethylamine hydrothiocyanate as a CuI crystal growth inhibitor. Langmuir 2002;18(26):10493–5.
[103] Heng L, Wang X, Yang N, Zhai J, Wan M, Jiang L. p–n-junction-based flexible dye-sensitized solar cells. Advanced Functional Materials 2010;20(2):266–71.
[104] Bach U, Lupo D, Comte P, Moser JE, Weissörtel F, Salbeck J, Spreitzer H, Grätzel M. Solid-state dye-sensitized mesoporous TiO_2 solar cells with high photon-to-electron conversion efficiencies. Nature 1998;395(6702):583–5.
[105] Kron G, Egerter T, Werner JH, Rau U. Electronic transport in dye-sensitized nanoporous TiO_2 solar cells—comparison of electrolyte and solid-state devices. Journal of Physical Chemistry B 2003;107(15):3556–64.
[106] Wang P, Zakeeruddin SM, Moser JE, Nazeeruddin MK, Sekiguchi T, Grätzel M. A stable quasi-solid-state dye-sensitized solar cell with an amphiphilic ruthenium sensitizer and polymer gel electrolyte. Nature Materials 2003;2(6):402–7.
[107] Wang P, Zakeeruddin SM, Comte P, Exnar I, Grätzel M. Gelation of ionic liquid-based electrolytes with silica nanoparticles for quasi-solid-state dye-sensitized solar cells. Journal of the American Chemical Society 2003;125(5):1166–7.
[108] Hardin BE, Hoke ET, Armstrong PB, Yum JH, Comte P, Torres T, Fréchet JMJ, Nazeeruddin MK, Grätzel M, McGehee MD. Increased light harvesting in dye-sensitized solar cells with energy relay dyes. Nature Photonics 2009;3(7):406–11.
[109] Wang B, Kerr LL. Dye sensitized solar cells on paper substrates. Solar Energy Materials and Solar Cells 2011;95(8):2531–5.
[110] Wang M, Anghel AM, Marsan B, Ha NLC, Pootrakulchote N, Zakeeruddin SM, Grätzel M. CoS supersedes Pt as efficient electrocatalyst for triiodide reduction in dye-sensitized solar cells. Journal of the American Chemical Society 2009;131(44)):15976–7.
[111] Kavan L, Yum JH, Grätzel M. Optically transparent cathode for dye-sensitized solar cells based on graphene nanoplatelets. Acs Nano 2011;5(1): 165–72.
[112] Nattestad A, Mozer AJ, Fischer MKR, Cheng YB, Mishra A, Bäuerle P, Bach U. Highly efficient photocathodes for dye-sensitized tandem solar cells. Nature Materials 2010;9(1):31–5.
[113] 〈http://www.sony.net/SonyInfo/technology/technology/theme/solar_01.html〉.